Calcified Tissue International
https://doi.org/10.1007/s00223-021-00831-6

ORIGINAL RESEARCH

Utilization of Mechanical Stress to Treat Osteoporosis: The Effects of Electrical Stimulation, Radial Extracorporeal Shock Wave, and Ultrasound on Experimental Osteoporosis in Ovariectomized Rats

Shota Inoue[1] · Junpei Hatakeyama[1] · Hitoshi Aoki[2] · Hiroshi Kuroki[3] · Takahiro Niikura[4] · Keisuke Oe[4] · Tomoaki Fukui[4] · Ryosuke Kuroda[4] · Toshihiro Akisue[5] · Hideki Moriyama[5]

Received: 6 October 2020 / Accepted: 24 February 2021

Abstract

Current treatment options for osteoporosis primarily involve pharmacotherapies, but they are often accompanied by undesirable side effects. Utilization of mechanical stress which can noninvasively induce bone formation has been suggested as an alternative to conventional treatments. Here, we examined the efficacy of mechanical stress induced by electrical stimulation, radial extracorporeal shock waves, and ultrasound for estrogen-deficient osteoporosis. Female Wistar rats were divided into following five groups: sham-operated group, untreated after ovariectomy, and treated with electrical stimulation, radial extracorporeal shock wave, or ultrasound starting at 8 weeks after ovariectomy for 4 weeks. Trabecular bone architecture of the femur was assessed by micro-CT and its biomechanical properties were obtained by mechanical testing. The femurs were further evaluated by histochemical, immunohistochemical, and real-time PCR analyses. Radial extracorporeal shock wave and ultrasound treatment improved trabecular bone microarchitecture and bone strength in osteoporotic rats, but not electrical stimulation. The shock wave decreased osteoclast activity and RANKL expression. The exposure of ultrasound increased osteoblast activity and β-catenin-positive cells, and they decreased sclerostin-positive osteocytes. These findings suggest that mechanical stress induced by radial extracorporeal shock wave and ultrasound can improve estrogen-deficient bone loss and bone fragility through promoted bone formation or attenuated bone resorption.

Keywords Mechanical stress · Electrical stimulation · Radial extracorporeal shock wave · Ultrasound · Osteoporosis

Introduction

Osteoporosis is a major public health concern worldwide. It is defined as a systemic skeletal disease characterized by low bone mass and a deterioration of bone microarchitecture, leading to enhanced bone fragility and increased fracture risk [1]. As fractures have severe impacts on quality of life and prognosis [2, 3], the prevention and treatment of osteoporosis can have great significance in affected patients. Current treatments for osteoporosis typically involve pharmacotherapy (e.g., bisphosphonates, teriparatide, and vitamin D supplementation) and exercise therapy. Although these drugs are effective as antiresorptive and anabolic agents, they have potentially negative side effects, such as osteonecrosis of the jaw, hypocalcemia, and atypical femoral fractures [4, 5]. Alternatively, physical exercise, particularly high-intensity resistance training [6], exerts mechanical stress on bone tissues, resulting in maintenance or gain of bone mass without any side effects [7]. However, high-intensity exercise is often

✉ Hideki Moriyama
morihide@harbor.kobe-u.ac.jp

1 Department of Rehabilitation Science, Graduate School of Health Sciences, Kobe University, Kobe, Japan

2 OG Wellness Technologies Co., Ltd, Okayama, Japan

3 Department of Physical Therapy, Human Health Sciences, Graduate School of Medicine, Kyoto University, Kyoto, Japan

4 Department of Orthopaedic Surgery, Kobe University Graduate School of Medicine, Kobe, Japan

5 Life and Medical Sciences Area, Health Sciences Discipline, Kobe University, Tomogaoka 7-10-2, Suma-ku, Kobe, Hyogo 654-0142, Japan

Published online: 22 March 2021

difficult for elderly patients due to a deterioration in physical fitness. These limitations of conventional therapies justify the search for alternative treatments for osteoporosis.

Mechanical stress plays a critical role in bone homeostasis, and mechanical loading induces bone formation and increases bone strength [8–10]. These point toward a possible therapeutic role for mechanical stress in the treatment for osteoporosis without side effects. We therefore focused on the utilization of mechanical stress induced by electrical stimulation, radial extracorporeal shock waves, and ultrasound as a promising new approach to treat osteoporosis.

Muscle contraction induced by electrical stimulation has been shown to prevent disuse-induced bone loss in rodents [11, 12]. However, to our knowledge, there are no reports on estrogen deficiency-induced bone loss. Thus, it remains unclear whether muscle contraction by electrical stimulation is effective for postmenopausal bone loss due to the differences in the pathogenesis mechanisms between disuse-induced and estrogen deficiency-induced osteoporosis [13].

Extracorporeal shock waves have proven effective against nonunion and fresh fractures [14, 15]. These experimental studies applied focused shock waves to a small area of tissue, while the skeletal sites that need to be treated for osteoporosis are larger. We therefore predicted that radial extracorporeal shock waves, which enable treatment of larger areas, are appropriate for treating osteoporosis. Only a few studies have investigated the effects of radial extracorporeal shock waves in osteoporotic animal [16, 17], and a human study did not show its protective effects on postmenopausal bone loss [18]. Thus, the effectiveness of the radial extracorporeal shock wave in osteoporosis and its optimal intensity for enhancing bone formation is poorly understood.

Low-intensity pulsed ultrasound (LIPUS), which provides mechanical stress through acoustic waves at intensity < 0.1 W/cm^2, is commonly used to promote fracture healing in clinical settings [19]. However, the effectiveness of LIPUS in treating osteoporosis is controversial with some studies suggesting therapeutic efficacy for bone loss in ovariectomized rats [20, 21] while other study [22] indicating treatment failure. Such positive effects in animal models have not been found in human osteoporosis after spinal cord injury [23] and menopause [24]. The lack of LIPUS efficacy in osteoporosis may be attributed to a lower mechanical stress of ultrasound due to a significant attenuation (20–40% of ultrasound energy) effect on the ultrasound translation [22–24]. Additionally, ultrasound signal intensity plays an important role in modulating the response of bone formation. Of 3 different intensities (0.005, 0.03, and 0.1 W/cm^2), ultrasound at only 0.1 W/cm^2 could prevent bone loss in ovariectomized rats [21]. Similarly, in vitro exposure of ultrasound at different intensities ranging from 0.002 to 0.03 W/cm^2 to rat bone marrow stromal cells enhanced the osteogenic differentiation in an ultrasound intensity-dependent manner [25]. Li et al. [26] also found that 0.6 or 1.2 W/cm^2 was optimal ultrasound intensities for osteoblast growth among the various intensities ranging from 0.15 to 2.4 W/cm^2. Based on these findings, we believe that a therapeutic potential of ultrasound is at higher intensity than LIPUS for osteoporosis; but to our knowledge, this has not been evaluated.

We examined the effects of mechanical stress induced by electrical stimulation, radial extracorporeal shock waves, and ultrasound on estrogen-deficient osteoporosis in ovariectomized rats. The goal of this study was to develop novel therapeutic approaches for osteoporosis, utilizing mechanical stress induced by physical agents as an alternative to conventional treatments.

Materials and Methods

Experimental Design

All experimental procedures were approved by our institutional animal care and use committee and according to the Kobe University Animal Experimentation Regulations (approval number: P160607). In total, 47 female Wistar retired breeder rats (5–6 months old, 250–350 g, Japan SLC Inc., Shizuoka, Japan) were used in this study.

Forty-two of these animals received bilateral ovariectomy to simulate postmenopausal osteoporosis [27], while 5 animals were sham-operated, meaning the operative procedure was the same except that the ovaries were left intact. After 8 weeks of ovariectomy or sham operation, the rats were randomly divided into following 5 groups: sham-operated group (control group, $n = 5$), untreated after ovariectomy (OVX group, $n = 4$), and treated with electrical stimulation (ES group), radial extracorporeal shock wave (rESW group), or ultrasound (US group) after ovariectomy. The animals in each treatment group were assigned 2 or 3 subgroups, corresponding to the stimulation intensity: 8 or 16 mA for ES group (ES-8 or -16 mA group, $n = 4$ per intensity); 1, 2, or 3 bar for rESW group (rESW-1, -2, or -3 bar group, $n = 5$ per intensity); 0.5, 1.0, or 1.5 W/cm^2 for US group (US-0.5, -1.0, or -1.5 W group, $n = 5$ per intensity). The rats were treated with each physical agent for 4 weeks after 8 weeks of ovariectomy. The rats were anesthetized for 7 days per week in the control, OVX, ES, and US groups and for 1 day per week in the rESW group throughout the 4-week treatment period. The animals were housed in pairs in polycarbonate cages with bedding and were maintained under artificial conditions at a constant temperature of 22 ± 1 °C with constant humidity of 55% ± 5% and a 12-h light–dark cycle. They were allowed free access to standard food and water 24 h a day.

Electrical Stimulation

Each rat received electrical stimulation for 10 min per day for 7 days per week over 4 weeks. Both hind legs of the rats were shaved, and the rats were anesthetized. The bilateral quadriceps in the ES groups were then electrically stimulated by paired gold surface electrodes (diameter 7 mm). The electrodes were connected to an electrical stimulator (ASPIA TS-1000; Nihon Medix, Chiba, Japan) to transmit a square pulse at a frequency of 10 Hz with two different intensities of 8 or 16 mA. A rest-insertion period (1 s contraction followed by 4 s rest) was added to avoid muscle fatigue.

Radial Extracorporeal Shock Wave

The rats in the rESW groups were treated with radial extracorporeal shock wave one weekly session for four times. Both hind legs of the anesthetized rat were shaved and an ultrasonic gel was applied, as coupling media. The rats were then placed on its right- or left-dorsal lateral side. The applicator, 1.5 cm in diameter, connected to the radial shock wave device (Physio-ShockMaster, SAKAI Medical Co., Ltd., Tokyo, Japan) was placed at the anterolateral side of the hind leg and covered distal half of the femur. Each femur was exposed to shock wave that consisted of a total of 2000 shock waves per treatment session at 5 Hz with three different intensities of 1, 2, or 3 bar.

Ultrasound

Bilateral femurs of each rat in the US groups were exposed to an ultrasound stimulation for 20 min for 7 days per week over 4 weeks. The bilateral hindlimbs of the rats were shaved and the ultrasound gel was applied. A type of plane circular transducer, 3.7 cm in diameter, with ultrasound device (SONICCTIZER, MINATO Medical Science Co., Ltd., Osaka, Japan) was then placed at the anterolateral side of the hind leg and covered whole of the femur. During treatment, the rats placed on its right- or left-dorsal lateral side under anesthesia. The signal was characterized by 200 µs pulses of 1.0 MHz sine wave with a pulse repetition frequency of 1 kHz and spatial-averaged temporal-averaged intensity (I_{SATA}) equal to 0.5, 1.0, or 1.5 W/cm^2.

Micro-computed Tomography (µCT)

At the end of the experimental period, all animals were euthanized by exsanguination under anesthesia. Bilateral femurs were harvested and stored at − 80 °C until they were analyzed. To scan the distal portions of the left femurs, micro 3D X-ray CT system (R_mCT2; Rigaku, Tokyo, Japan) with an isotropic voxel resolution of 20 µm was employed at a voltage 90 kV, current of 160 µA, and a scan time of 3 min per sample. For assessment of changes in trabecular and cortical bone in the femoral metaphysis, 3D image reconstruction and data processing were completed with TRI/3D-BON software (Ratoc, Tokyo, Japan). A region of interest was manually selected for the analysis of trabecular and cortical bone microarchitecture, which was 750 µm long in the distal femoral metaphysis directly above the growth plate, excluding the growth plate as described previously [11]. Trabecular and cortical bone were automatically separated using software with thresholds of 650 mg HA/cm^3 for trabecular bone or 750 mg HA/cm^3 for cortical bone. Trabecular architecture was characterized by determining trabecular bone volume fraction (BV/TV), trabecular thickness (Tb.Th), trabecular number (Tb.N), trabecular separation (Tb.Sp), and bone mineral content-to-tissue volume ratio (BMC/TV). Cortical architecture was characterized by cortical thickness (Ct) and cortical volume to all tissue volume (Cv/Av).

Biomechanical Testing

The functional mechanical properties of the distal femoral metaphysis were assessed by a compression test as previously described for the tibial metaphysis [28]. After the µCT scanning, the left femurs were placed with the stable three-point contact on the base. The base was fixed in a mechanical testing system (AUTOGRAPH, Shimadzu, Kyoto, Japan) with distance of exactly 5 mm between the end of the distal femur and the center of the roller stamp. A 1 N preload was applied to the ventral aspect of the condyles and then compressed at a speed of 10 mm/min until the fracture occurred. The maximum load, energy to failure, and stiffness were obtained from the load–deflection curve and determined as the strength of the distal femur.

Histology

Histological Preparation

Nondemineralized frozen sections were prepared according to the method described by Kawamoto [29]. Briefly, the right femur was freeze-embedded with super cryoembedding medium (SCEM, Leica Microsystems, Tokyo, Japan) in isopentane at − 75 °C. Cross sections of the femur in the coronal plane (5 µm thick) were cut from each sample, and were then used for histochemical or immunohistochemical analyses.

Histochemical and Histological Analysis

To detect alkaline phosphatase (ALP) and tartrate-resistant acid phosphatase (TRAP) activity, tissue sections were stained with TRAP/ALP stain kit (Wako Pure Chemical,

Osaka, Japan), respectively, according to the manufacturers' instructions. For histomorphometric analysis, four random fields of view per sample/rat were randomly taken from 1000 μm long directly above the growth plate in the distal femoral metaphysis with a light microscope (BX53; Olympus, Tokyo, Japan) and a camera (DP73; Olympus) at a magnification of 20X. Osteoblast surface was measured manually using Image J 1.50 (National Institutes of Health, Bethesda, MD, USA) as the total length of ALP-positive surface divided by bone surface. Osteoclast surface was similarly analyzed following TRAP staining.

Osteocyte density and viability were measured on the sections stained with hematoxylin and eosin. The trabecular area was measured using the same method as for the bone surface, and living and dying/dead cells were counted manually. The living cells were characterized by a whole nucleus with no empty space in the lacuna. The dying/dead cells were morphologically identified as either a fragmented nucleus, a small polarized nucleus, or no hematoxylin-stained material in the lacuna [30]. Osteocyte density and osteocyte death were determined as the number of living cells and dying/dead cells per trabecular area (mm^2), respectively.

Immunohistochemistry

Immunohistochemistry was conducted following protocols established in our laboratory [31]. Briefly, the frozen sections of 5 μm thick of the femurs were fixed in 100% ethanol for 2 min and 4% paraformaldehyde/0.01 M phosphate-buffered saline ([PBS], pH 7.4) for 2 min, and decalcified in 10% ethylenediaminetetraacetic acid (EDTA) for 1 h. The sections were then incubated with mouse monoclonal anti-type I collagen (diluted 1:4000; C2456, Sigma-Aldrich, St. Louis, MO, USA), goat polyclonal anti-sclerostin (diluted 1:400; AF1589, R&D Systems, Minneapolis, MN, USA), rabbit monoclonal anti-β-catenin (diluted 1:200; ab32572, Abcam, Tokyo, Japan), and goat polyclonal anti-receptor activator of nuclear factor kappa-B ligand (RANKL; diluted 1:20; sc-7628, Santa Cruz, Dallas, TX, USA) antibodies at 4 °C overnight. A subsequent reaction was made by the streptavidin–biotin-peroxidase complex technique using Elite ABC kit (diluted 1:50; PK-6100; Vector Lab., Burlingame, CA, USA). Immunoreactivity was visualized by adding diaminobenzidine tetrahydrochloride reagent (ImmPACT™ DAB peroxidase substrate kit, SK-410, Vector Lab.). Finally, the sections were counterstained Mayer's hematoxylin. The immunolabeled sections were captured in four random trabecular regions from 1000 μm long directly above the growth plate in the distal femoral metaphysis with the light microscope (BX53; Olympus) and the camera (DP73; Olympus) at a magnification of 20X.

For type I collagen, histological images were converted to grayscale images with Adobe Photoshop CS2 (Adobe Systems, San Jose, CA, USA). The mean of pixel gray values (in the range 0–255) in trabecular bone was measured with Image J 1.50 (National Institutes of Health). Staining intensity was calculated with the following formula: Staining intensity = 255 – mean gray value [32]. For sclerostin, the number of sclerostin-positive and total osteocytes was manually counted and expressed as the ratio of number of positive osteocytes/total osteocytes. For RANKL and β-catenin, the number of positive cells in the trabecular surface was manually counted and expressed as the number of positive cells/bone perimeter (mm).

RNA Extraction and Real-Time Polymerase Chain Reaction (PCR)

We evaluated the mRNA expression level of sclerostin, receptor activator of nuclear factor-κB ligand (RANKL), and osteoprotegerin (OPG) in the femur. Total RNA of the femur was extracted from frozen sections by slightly modifying the protocol for the joint capsule [33]. After cutting the histological sections, 50 μm frozen sections of the femur were prepared from the same samples, and the bone tissue in the femoral metaphysis (0 to 2000 μm away from growth plate) was isolated using tweezers, under a stereomicroscope. Total RNA was then extracted with the RNeasy Plus Universal Mini kit (Qiagen, Hilden, Germany) according to the manufacturer's protocols. Quality of the isolated RNA was checked by measuring OD 260/280 with BioPhotometer D30 (Eppendorf, Hamburg, Germany).

Reverse transcription was performed using total RNA and the TaqMan™ Fast Virus 1-Step Master Mix (Thermo Fisher Scientific, Waltham, MA, USA). RT-PCR reactions were conducted using Step One Real-Time PCR System (Applied Biosystems, Foster City, CA, USA) with TaqMan gene expression assays (Applied Biosystems) for sclerostin (Sost: Rn00577971_m1), RANKL (Tnfsf11: Rn00589289_m1), OPG (Tnfrsf11b: Rn00563499_m1), and GAPDH (Gapdh: Rn01775763_g1). Gapdh was used as an internal control for calculating the relative expression of each target gene by using the $2^{-\Delta\Delta Ct}$ method [34].

Statistical Analysis

Statistical analyses were conducted with R (version 3.6.1, R Foundation for Statistical Computing, Vienna, Austria). Descriptive statistics were calculated as median and interquartile range. An alpha level of 0.05 was used for all statistical tests, and two-tailed tests were applied. The Kruskal–Wallis nonparametric test was used to evaluate the differences among the groups. When statistical significance was achieved, a post hoc Welch test was used to further

specify the difference between the groups. For the post hoc analysis, the Shaffer correction was applied to adjust the a priori alpha level to the number of comparisons performed. A post hoc power analysis for the Kruskal–Wallis test by G*Power 3 program [35] was used to confirm that sufficient number of animals had been used (Supplementary Table S1).

Results

Body Weight

Body weight in ovariectomized rats increased after 8 weeks of ovariectomy compared to the control group ($P < 0.05$) (Supplementary Table S2). However, there was no difference in body weight among the groups after 12 weeks of ovariectomy.

Bone Microarchitecture

Trabecular bone mass in the distal femur was reduced in ovariectomized rats (Fig. 1), as confirmed by decreased BV/TV, Tb.N, and BMC/TV and increased Tb.Sp in the OVX group compared to the control group ($P < 0.01$) (Table 1). Tb.Th did not change significantly by ovariectomy ($P > 0.05$). There were no significant differences in these parameters between the OVX group and the ES-8 and ES-16 mA groups. However, in ovariectomized rats that received extracorporeal shock wave, Tb.Sp decreased in the rESW-2 and rESW-3 bar group compared with the OVX group ($P < 0.05$). In ovariectomized rats that received ultrasound, BV/TV and Tb.N were larger and Tb.Sp was less in the US-1.5 W group than in the OVX group ($P < 0.05$). Furthermore, in the US-1.5 W group, BV/TV was larger than in the US-0.5 and US-1.0 W groups ($P < 0.05$). BV/TV

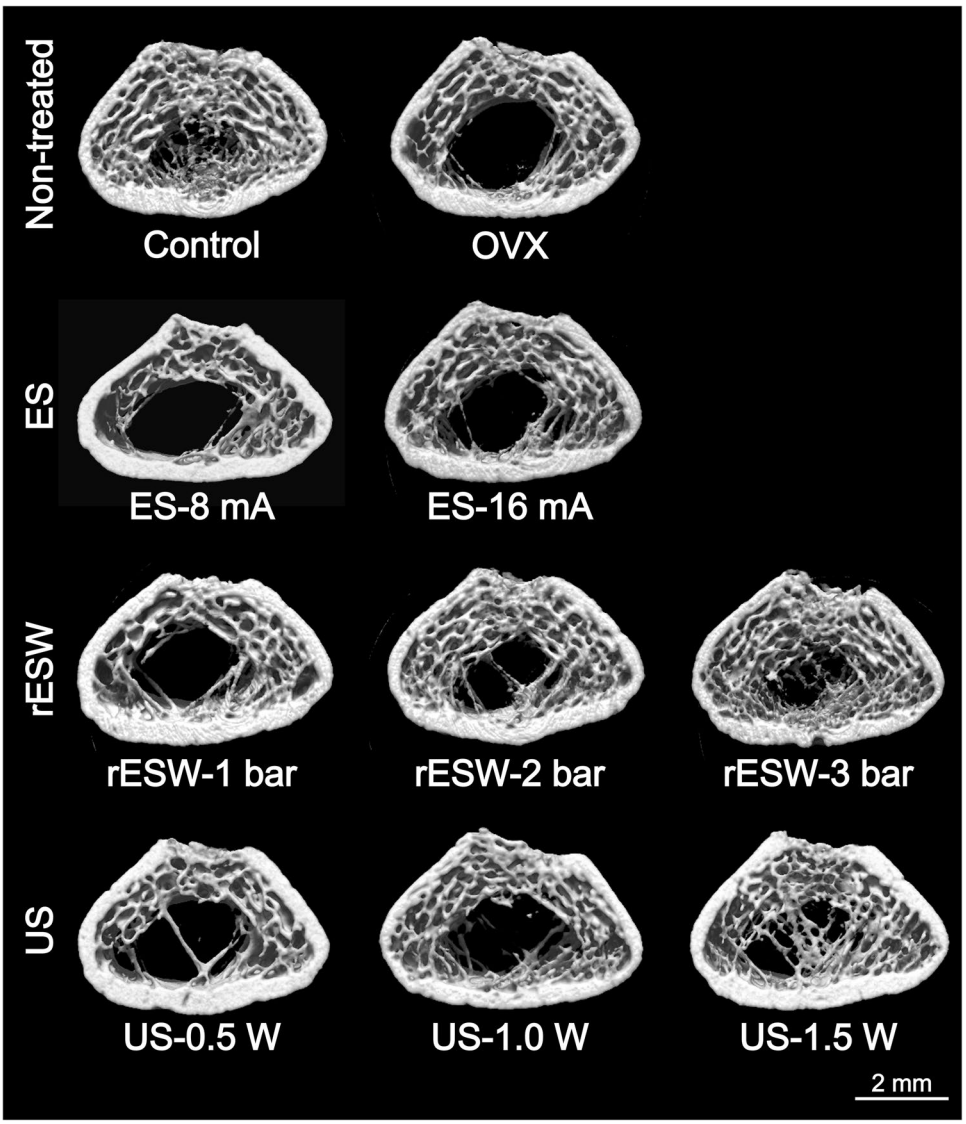

Fig. 1 Representative 3D images of the distal femur obtained by μCT analysis. Scale bar = 2 mm. *OVX* ovariectomy, *ES* electrical stimulation, *rESW* radial extracorporeal shock wave, *US* ultrasound

Table 1 Trabecular and cortical bone microarchitecture of distal femur quantified by μCT

	Control	OVX	Electrical stimulation		Radial extracorporeal shock wave			Ultrasound		
			ES-8 mA	ES-16 mA	rESW-1 bar	rESW-2 bar	rESW-3 bar	US-0.5 W	US-1.0 W	US-1.5 W
BV/TV (%)	14.4 (13.4, 18.1)	7.9 (7.7, 8.4)*	10.7 (10.2, 10.9)*	11.0 (10.5, 11.9)	11.0 (10.2, 11.5)*	11.6 (10.1, 13.0)	12.4 (12.2, 13.0)	10.5 (9.6, 10.6)*	10.2 (7.9, 11.3)*	13.8 (13.6, 13.9)[a,b]
Tb.Th (μm)	55.5 (54.0, 56.2)	50.9 (50.3, 52.0)	50.2 (45.7, 54.5)	53.9 (52.9, 54.7)	54.2 (49.2, 54.3)	55.2 (51.1, 55.6)	53.5 (53.4, 59.0)	48.1 (46.4, 49.5)	45.3 (45.1, 51.7)	50.5 (49.6, 57.6)
Tb.N (1/μm)	2.7 (2.4, 3.2)	1.6 (1.5, 1.8)*	2.0 (2.0, 2.1)	2.0 (1.9, 2.3)	2.0 (1.9, 2.2)	2.1 (2.0, 2.4)	2.3 (2.2, 2.4)	2.1 (1.9, 2.2)	2.2 (1.8, 2.2)	2.4 (2.3, 2.8)[a]
Tb.Sp (μm)	321.0 (256.0, 363.4)	601.0 (579.5, 616.3)*	443.1 (424.0, 449.7)	437.4 (396.2, 467.6)	439.7 (409.1, 477.3)	423.8 (370.2, 445.6)[a]	379.3 (365.1, 397.3)[a]	433.8 (412.0, 465.0)	404.1 (399.3, 525.3)	356.4 (309.3, 367.4)[a]
BMC/TV (mg/cm^3)	164.0 (149.8, 183.1)	80.0 (76.6, 82.1)*	91.7 (86.4, 93.4)*	93.7 (89.7, 101.7)*	95.9 (95.6, 100.3)	101.3 (84.1, 109.6)*	104.5 (101.7, 111.1)*	86.1 (84.3, 90.7)*	97.6 (72.5, 118.7)*	117.7 (114.2, 121.0)
Ct (μm)	426.1 (420.0, 431.0)	406.7 (399.7, 417.5)	434.3 (416.7, 447.3)	418.4 (410.4, 427.7)	403.3 (402.2, 403.3)	400.9 (393.7, 411.9)	409.1 (408.5, 416.8)	419.1 (413.3, 429.9)	439.7 (429.8, 442.7)	440.9 (423.5, 449.9)
Cv/Av (%)	38.6 (37.5, 39.9)	37.1 (35.7, 38.6)	39.5 (38.8, 40.7)	39.2 (38.5, 39.8)	37.4 (36.8, 39.2)	37.4 (36.9, 37.9)	37.9 (36.9, 39.1)	38.4 (38.4, 38.6)	38.8 (37.4, 39.9)	39.5 (39.0, 40.8)

Displacement values are given as median (interquartile range)

*$P < 0.05$ vs. control group

[a]$P < 0.05$ vs. OVX group

[b]$P < 0.05$ vs. US-0.5 and US-1.0 W group

OVX ovariectomy, *BV/TV* trabecular bone volume/tissue volume, *Tb.Th* trabecular bone thickness, *Tb.N* trabecular bone number, *Tb.Sp* trabecular bone separation, *BMC/TV* bone mineral content/tissue volume, *Ct* cortical thickness, *Cv/Av*, cortical volume/all tissue volume

in the US-1.5 W group recovered to the same level as that in the control group ($P = 1.00$, US-1.5 W group vs. control group). The cortical architecture of the distal femur, which is characterized by Ct and Cv/Av, showed no differences among all groups ($P > 0.05$).

Biomechanical Properties

As shown in Fig. 2, ovariectomy resulted in significantly less maximal load than in the control group ($P < 0.05$). Maximum load was tended to be higher in the US-1.5 W groups than in the OVX group, but no significant difference was detected ($P = 0.15$) (Fig. 2a). Energy to failure in the rESW-2 and rESW-3 bar and US-1.5 W groups were increased compared with the OVX group ($P < 0.05$) (Fig. 2b). Stiffness showed no differences between the OVX and each treatment group ($P > 0.05$) (Fig. 2c).

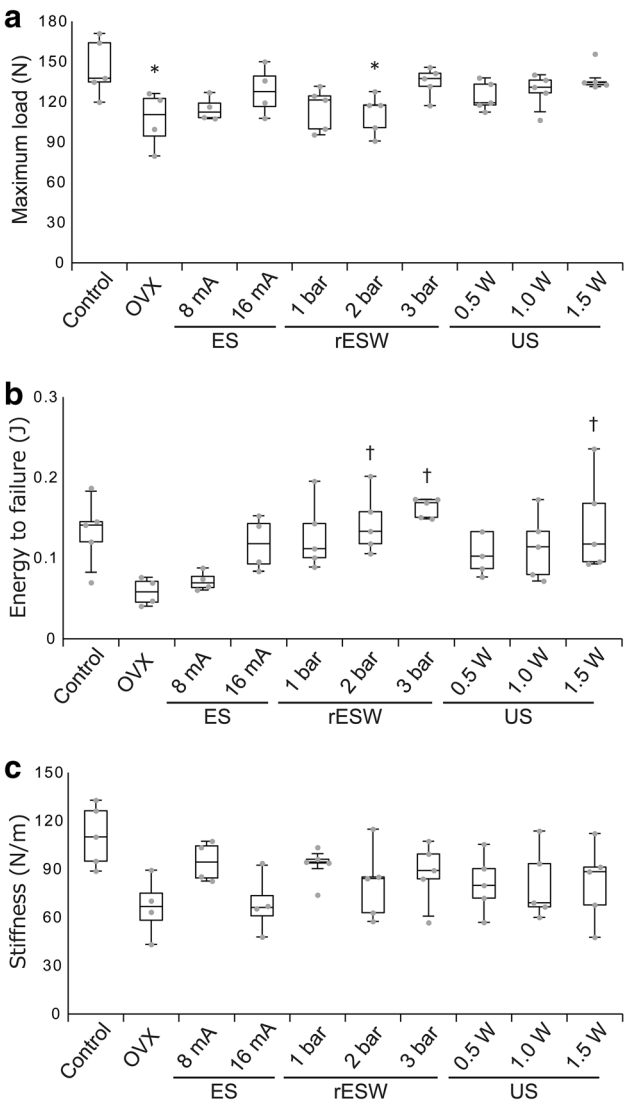

Fig. 2 The graphs show **a** maximum load, **b** energy to failure, and **c** stiffness evaluated by the compression test for the distal metaphysis. The horizontal bars indicate the median and the vertical bars the range. The horizontal boundaries of the boxes represent the first and third quartiles. Dot plots represent individual data. *$P < 0.05$ vs. control group; †$P < 0.05$ vs. OVX group. *OVX* ovariectomy, *ES* electrical stimulation, *rESW* radial extracorporeal shock wave, *US* ultrasound

Osteoblast and Osteoclast Activity

ALP staining as an indicator of osteoblastic activity in the trabecular bone surface showed more ALP-positive regions in the rESW and US groups than that in the control or OVX groups (Fig. 3a). TRAP staining revealed the localization of osteoclast in the trabecular bone (Fig. 3b). Percentage of osteoblast surface was markedly increased in the US-1.5 W groups when compared to the control group ($P < 0.05$) (Fig. 3c). Additionally, the percentage was greater in the US-1.5 W group than that in the US-0.5 W groups ($P < 0.05$). Percentage of osteoclast surface was increased after ovariectomy ($P < 0.05$ vs. control group) and reduced by shock wave at intensity of 2 bar ($P < 0.05$ vs. OVX group) (Fig. 3d).

Osteocyte Density and Osteocyte Death

Osteocyte density was comparable among the groups (Fig. 4a and b). On the other hand, the ovariectomized rats showed more lacunae with a small polarized or absent nucleus than the other groups. The number of dead osteocytes increased in the ovariectomized rats compared with the control rats ($P < 0.05$) (Fig. 4c). Furthermore, the dead osteocytes were greater in the rESW group than those in the US group ($P < 0.05$).

Immunohistochemical Analysis

As disclosed by immunohistochemistry, type I collagen was evenly distributed in the trabecular bone (Fig. 5a), and the staining intensity showed no differences among the groups (Table 2). Immunohistochemistry revealed protein expression of sclerostin at osteocytes (Fig. 5b). The US-1.5 W groups showed significant decrease in the sclerostin-positive osteocytes compared with the OVX group ($P < 0.05$) (Table 2). The immunolabeling of β-catenin was observed at the trabecular surface in all groups (Fig. 5c). The number of β-catenin-positive cells increased in the US-1.5 W group compared with the OVX and US-0.5 and US-1.0 W groups ($P < 0.05$) (Table 2). The RANKL-positive cells were observed at the trabecular surface, but not osteocytes (Fig. 5d). The number of RANKL-positive cells at the trabecular surface increased in the OVX group ($P < 0.05$ vs.

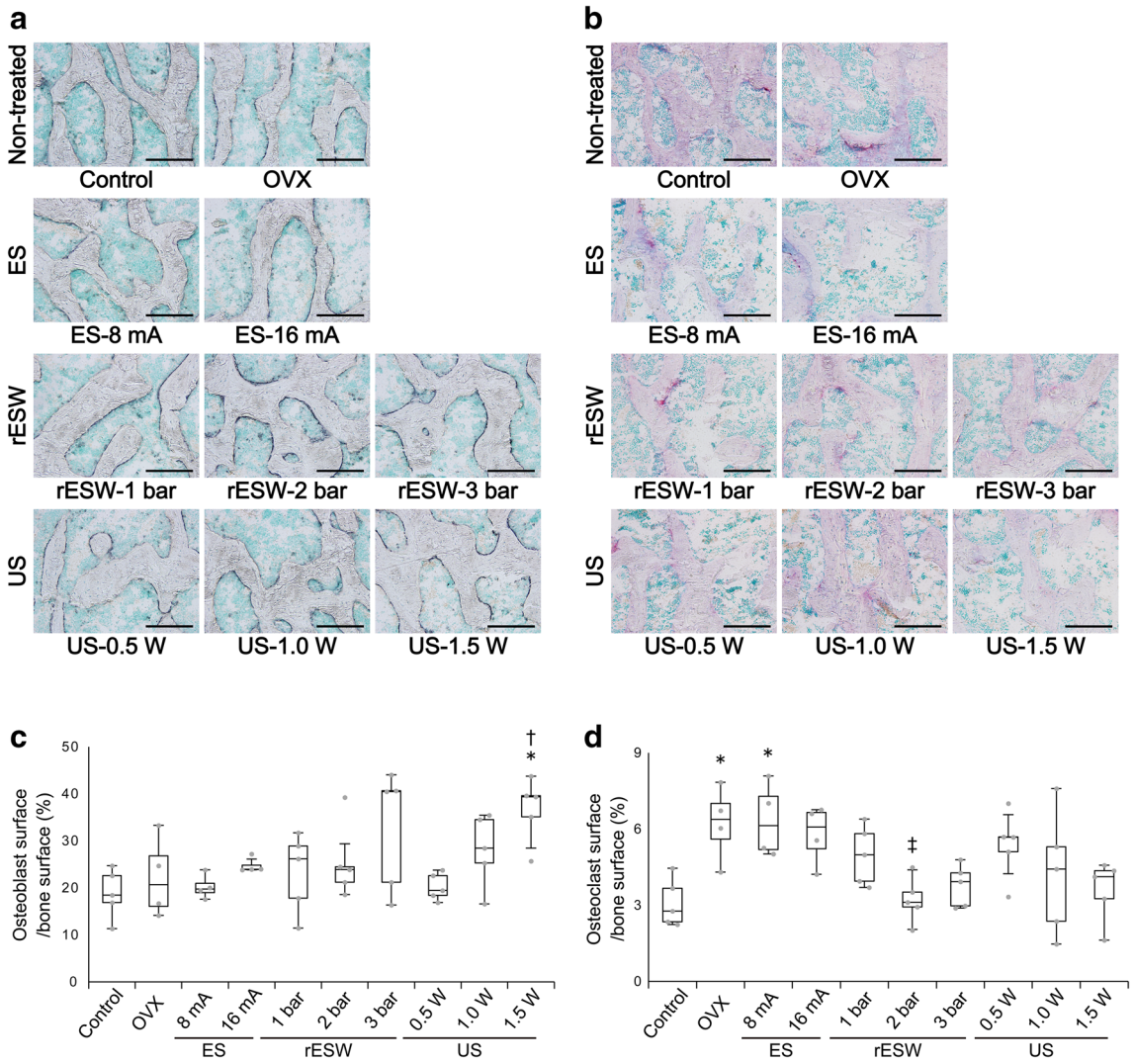

Fig. 3 Representative histological images in the femoral trabecular bone stained with **a** ALP and **b** TRAP. Scale bars = 200 µm. **c** Quantification of the ALP staining by osteoblast surface per trabecular bone surface. **d** Quantification of the TRAP staining by osteoclast surface per trabecular bone surface. The horizontal bars indicate the median and the vertical bars the range. The horizontal boundaries of the boxes represent the first and third quartiles. Dot plots represent individual data. *$P < 0.05$ vs. control group; †$P < 0.05$ vs. US-0.5 W group; ‡$P < 0.05$ vs. OVX group. *OVX* ovariectomy, *ES* electrical stimulation, *rESW* radial extracorporeal shock wave, *US* ultrasound

control group), but decreased in the US-1.0 and US-1.5 W groups compared with the OVX group ($P < 0.05$) (Table 2).

Changes in Gene Expression

The mRNA expressions in the distal femur were quantified by real-time PCR. The sclerostin mRNA expression showed no differences among all groups ($P > 0.05$) (Fig. 6a). The expression of RANKL mRNA was increased after ovariectomy ($P < 0.05$ vs. control group), and decreased in the rESW-3 bar and US-1.5 W groups when compared to the OVX group ($P < 0.05$) (Fig. 6b). The expression of OPG mRNA showed no differences among all groups (Fig. 6c). RANKL/OPG ratio was increased in the ES-8 mA group compared with the control group ($P < 0.05$) (Fig. 6d). Its ratio showed no differences between the untreated and treated groups.

Discussion

We examined the effects of mechanical stress induced by electrical stimulation, radial extracorporeal shock wave, and ultrasound on osteoporosis in ovariectomized rats. As a result, radial extracorporeal shock wave and ultrasound treatment improved trabecular bone microarchitecture and bone strength in osteoporotic rats. These treatments increased osteoblast activity or decreased osteoclast activity at the

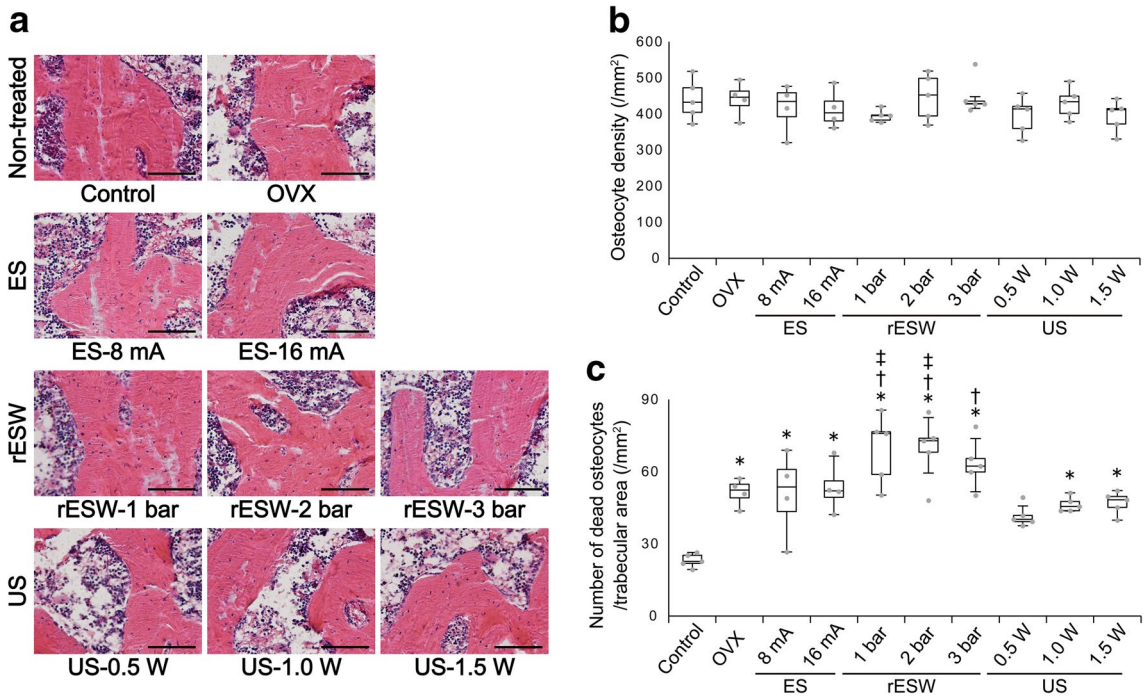

Fig. 4 **a** Representative histological images in the femoral trabecular bone stained with hematoxylin and eosin. Scale bars = 100 μm. **b** Osteocyte density in the trabecular bone. **c** The number of dead osteocytes per trabecular area (mm^2). The horizontal bars indicate the median and the vertical bars the range. The horizontal boundaries of the boxes represent the first and third quartiles. Dot plots represent individual data. *$P < 0.05$ vs. control group; †$P < 0.05$ vs. US-0.5 W group; ‡$P < 0.05$ vs. US-1.0 and US-1.5 W group. *OVX* ovariectomy, *ES* electrical stimulation, *rESW* radial extracorporeal shock wave, *US* ultrasound

trabecular bone surface. Suppression of RANKL may be responsible for its osteoclast inactivation in trabecular bone. Additionally, ultrasound reduced sclerostin protein level suggesting that mechanical stress induced by physical agents may contribute to the osteoblast activation.

In line with a previous report [36], ovariectomy markedly increased body weight after 8 weeks of surgery, but ovariectomy-induced weight gain was abolished after 12 weeks. This weight gain has been shown to persist through 12 weeks of ovariectomy [36]. Hence, the loss of weight gain between 8 and 12 weeks postoperatively might be due to daily anesthesia. However, there were no differences in body weight among each group at the end of the 4-week intervention. These results suggest that the difference in treatment types and the amount of anesthesia throughout the intervention period did not have a significant impact on animal wellness.

Postmenopausal osteoporosis leads to bone loss and the deterioration of bone microarchitecture due to the imbalance between bone formation and bone resorption after estrogen withdrawal [37]. In our study, ovariectomy-induced estrogen deficiency decreased the trabecular bone mass and impaired its microarchitecture in the distal femur decreased at 12 weeks after ovariectomy. Extracorporeal shock wave at 3 bar decreased trabecular separation when compared to the ovariectomized rat, indicating that its treatment improved bone microarchitecture caused by estrogen deficiency. This is consistent with the previous studies showing the effectiveness of radial extracorporeal shock wave in osteoporosis in a similar model [16, 17]. No reports have been available regarding the differences in shock wave intensity that stimulates bone formation, but our results indicate optimal intensities of 2 and 3 bar for improving bone microarchitecture in estrogen-deficient animals. Some studies have reported that ultrasound exposure at higher intensity promotes bone formation and osteoblast differentiation in vivo [21] and in vitro [25, 26]. We also found that the rats treated with ultrasound at 1.5 W/cm^2 had greater trabecular bone mass than the rats treated with 0.5 and 1.0 W/cm^2 implying ultrasound intensity-dependent improvement in bone mass. Unlike previous studies showing the inhibitory effects of LIPUS at 0.03 W/cm^2 on bone loss after ovariectomy [20, 21], in our study ultrasound exposure at 1.5 W/cm^2 increased bone mass, but not at 0.5 or 1.0 W/cm^2. In these previous studies, ultrasound was applied immediately after ovariectomy (0–7 days), whereas we started ultrasound treatment from 8 weeks post ovariectomy when the significant bone loss had been detected. Consequently, ultrasound exposure as a therapeutic strategy for osteoporosis may require at least 1.5 W/cm^2 of intensity.

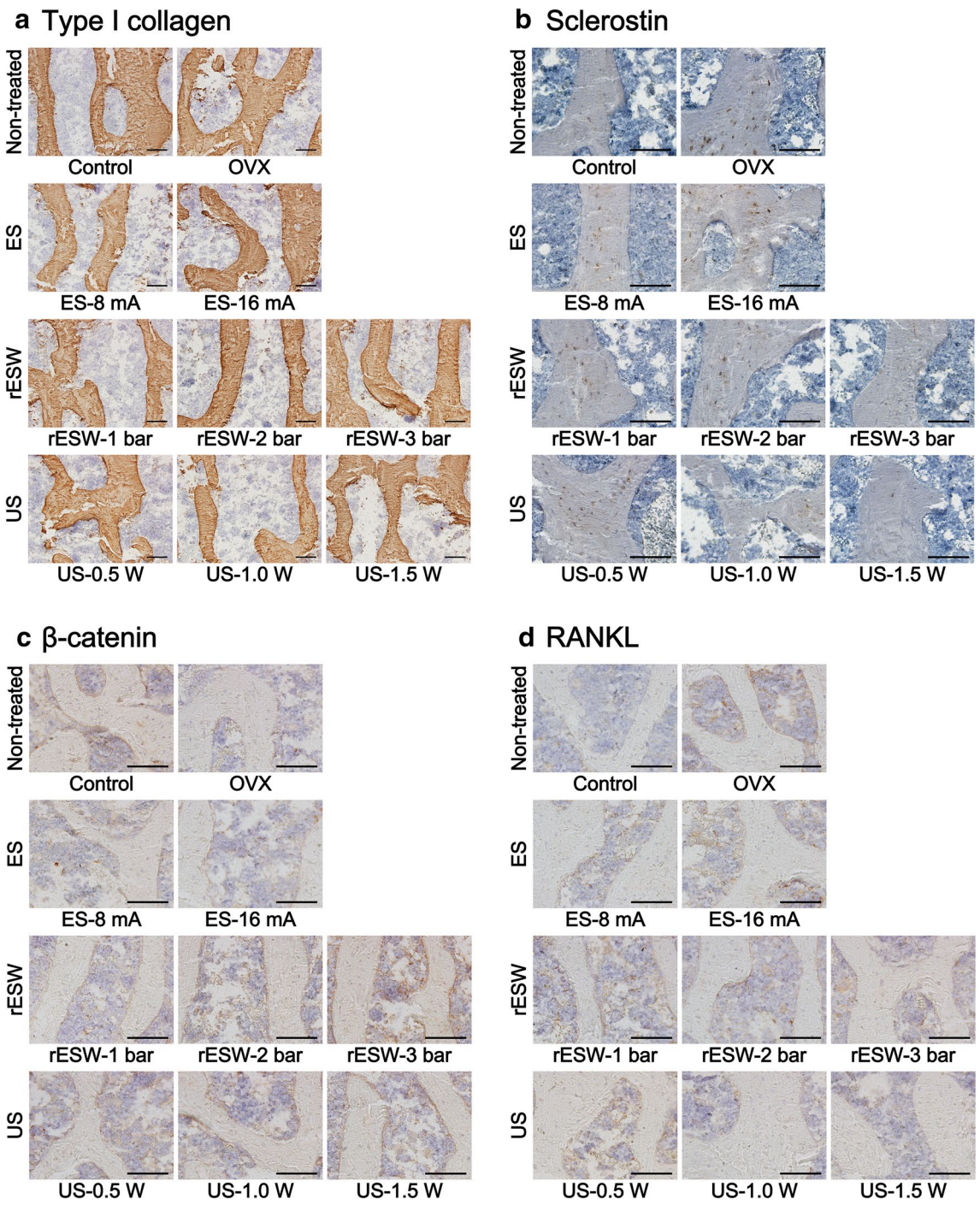

Fig. 5 Representative histological images in the femoral trabecular bone stained with **a** Type I collagen, **b** sclerostin, **c** β-catenin, and **d** RANKL. Scale bars = 100 μm. *OVX* ovariectomy; *ES* electrical stimulation, *rESW* radial extracorporeal shock wave, *US* ultrasound

Although extracorporeal shock wave and ultrasound increased the bone mass, electrical stimulation did not affect bone mass or microarchitecture. Some animal studies of bone loss caused by hindlimb unloading have reported the increase in bone mass by electrically induced muscle contraction [11, 12]. Bone is adapted to a customary mechanical environment, making them less responsive to mechanical stress if it does not exceed routine loading signals [9]. Contrary to the disuse-induced osteoporosis rat, the hindlimbs of the ovariectomized rat were subjected to weight loading. Thus, mechanical stress induced by electrical stimulation may be insufficient to induce bone adaptation.

Table 2 Quantification of immunohistochemical analyses

	Control	OVX	Electrical stimulation		Radial extracorporeal shock wave			Ultrasound		
			ES-8 mA	ES-16 mA	rESW-1 bar	rESW-2 bar	rESW-3 bar	US-0.5 W	US-1.0 W	US-1.5 W
Staining Intensity for Type I collagen	89.1 (88.8, 104.1)	100.0 (93.7, 101.5)	89.1 (85.0, 93.4)	100.6 (98.9, 101.3)	100.7 (93.4, 102.0)	103.4 (100.7, 105.1)	96.7 (94.6, 97.3)	91.4 (90.4, 95.4)	96.6 (96.4, 96.9)	101.7 (98.2, 110.0)
Sclerostin-positive osteocytes (%)	24.3 (19.2, 33.1)	38.4 (37.4, 39.4)	31.3 (29.3, 35.2)	32.2 (29.4, 33.7)	33.2 (31.2, 35.2)	30.4 (25.9, 36.4)	30.6 (22.1, 31.7)	35.2 (31.0, 39.3)	30.7 (26.8, 32.0)	23.6 (20.0, 28.6)[a]
β-catenin-positive cells/bone perimeter (/mm)	10.7 (8.8, 11.4)	7.2 (6.3, 7.7)	7.1 (5.8, 8.0)	7.0 (5.7, 8.3)	6.3 (5.8, 6.7)	7.9 (6.0, 8.6)	12.7 (10.4, 13.7)[b]	8.8 (7.6, 9.2)	5.9 (5.4, 8.3)	13.9 (12.6, 15.4)[a,c]
RANKL-positive cells/bone perimeter (/mm)	1.5 (1.4, 2.3)	3.7 (3.3, 4.2)*	3.7 (2.9, 4.3)	3.4 (3.0, 3.8)	3.7 (3.7, 4.0)*	3.4 (2.7, 3.6)	1.9 (1.8, 3.4)	2.4 (1.8, 3.1)	1.9 (1.3, 2.1)[a]	1.9 (1.9, 2.0)[a]

Displacement values are given as median (interquartile range)

*$P < 0.05$ vs. control group

[a]$P < 0.05$ vs. OVX group

[b]$P < 0.05$ vs. rESW-1 bar

[c]$P < 0.05$ vs. US-0.5 and US-1.0 W group

OVX ovariectomy

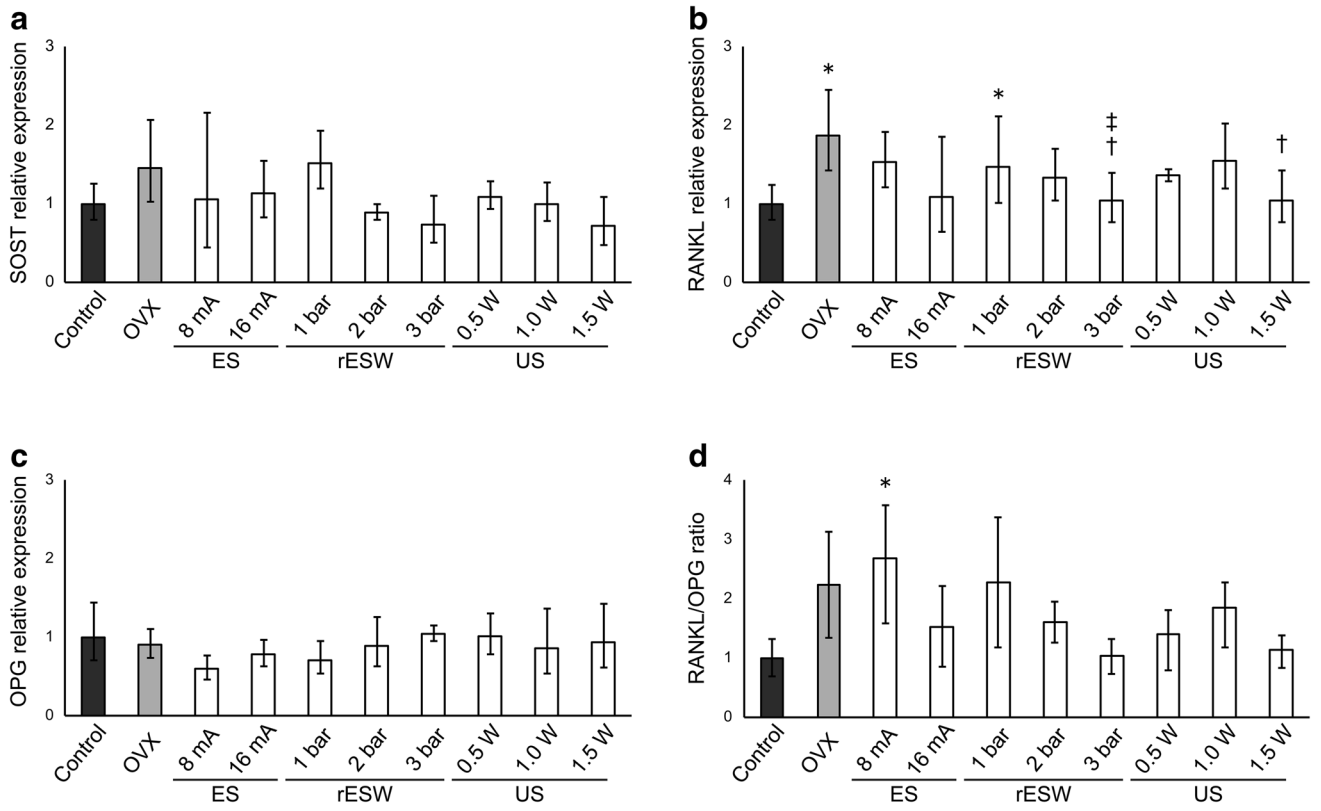

Fig. 6 The graphs show the relative mRNA expression of **a** SOST, **b** RANKL, and **c** OPG in the distal femur, and **d** RANKL/OPG ratio. Data are expressed as mean ± SD. *$P < 0.05$ vs. control group; †$P < 0.05$ vs. OVX group; ‡$P < 0.05$ vs. rESW-1 bar group. *OVX* ovariectomy, *ES* electrical stimulation, *rESW* radial extracorporeal shock wave, *US* ultrasound

It is well known that osteoporosis primarily affects the trabecular bone in the metaphysis of long bones, resulting in bone weakness [38]. Nevertheless, most of the experimental animal studies have evaluated the bone strength by three-point bending tests in the diaphysis of the femur or tibia [39]. We therefore chose the distal femoral metaphysis for the mechanical testing [28] and were able to show changes in the maximum load between the sham and ovariectomy rats. Although ovariectomy did not decrease the energy to failure, extracorporeal shock wave at 2 and 3 bar and ultrasound at 1.5 W/cm^2 increased it, suggesting that these treatments increased the trabecular bone leading to an increase in bone strength.

Estrogen deficiency affects bone turnover, including a temporary increase in osteoblasts and marked osteoclast activation [40]. After ovariectomy, osteoblasts initially increase with rapid increases in osteoclasts and thereafter gradually decrease, and consequently reach a plateau at 90 days [40]. At 12 weeks after ovariectomy, we also observed similar activity of ALP which is an osteoblastic differentiation marker [41] between the sham and ovariectomized rats, indicating that the osteoblastic activity reached a plateau. However, ALP activity was higher than in the ovariectomized rats at 12 weeks after ovariectomy in the rats received ultrasound. These results suggest that ultrasound persistently stimulate osteoblasts and increase bone formation. Consistent with a previous study [40], ovariectomy showed a marked increase in TRAP activity, a marker for osteoclast [42], at 12 weeks. However, extracorporeal shock wave decreased their activity to the same level as that of the untreated rats. These findings indicate that extracorporeal shock wave may reduce the increase in the osteoclast activity induced by estrogen deficiency, resulting in reduced bone resorption. RANKL is known to be key molecules in the regulation of osteoclast differentiation and activity [43]. Ovariectomy increased the protein level and mRNA expression of RANKL in the bone, and extracorporeal shock wave decreased them. Thus, RANKL suppression may contribute to osteoclast inactivation at trabecular bone in the rats treated with extracorporeal shock wave.

Osteocytes function as sensory cells that respond to mechanical loading and regulate both bone formation and bone resorption [44], and estrogen plays an important role in the maintenance of its viability [45]. Consistent with previous findings [46], ovariectomy-induced estrogen deficiency increased osteocyte death, but physical agents were unable

to prevent its death. Furthermore, the rats treated with the shock wave showed more osteocyte death than those treated with ultrasound. Osteocyte apoptosis can occur at sites of microdamage [47], and it is suggested that the osteogenic effects of the shock wave are triggered by microdamage [48]. Hence, the increase in osteocyte death after the shock wave treatment may be associated with the microdamage required to promote bone formation.

Sclerostin which is highly expressed in osteocytes has been defined as the key protein involved in mechanical stress [49], and its expression decreased by mechanical loading [10]. Ultrasound at intensity of 1.5 W/cm^2 decreased the sclerostin-positive osteocytes compared to the untreated group. Additionally, sclerostin acts as a negative regulator of bone formation by antagonizing Wnt/β-catenin signaling which plays an important role in osteoblast differentiation and activity [49]. In our study, the exposure of ultrasound increased the number of β-catenin-positive cells, suggesting that its treatment activates Wnt/β-catenin signaling. Therefore, the decrease in the expression of sclerostin in osteocytes in this study may partly contribute to osteoblast activation through Wnt/β-catenin activation. On the other hand, the number of sclerostin-positive osteocytes and the sclerostin mRNA expression were unaffected by electrical stimulation. Because mechanical stress modulates the expression of sclerostin in a magnitude-dependent manner [10], mechanical stress by electrical stimulation may be insufficient to affect the sclerostin levels in osteocytes. Taken together, our findings suggest that ultrasound increased osteoblast activity, at least in part, via downregulation of sclerostin thorough mechanical stress.

This study had several limitations. First, we used a small animal model. Wistar rats cannot fully reflect the variability found in humans; therefore our results may not be directly applicable to patients with osteoporosis. However, the ovariectomized rat model has been widely used in preliminary studies of postmenopausal osteoporosis [13]. Soft tissues in human are thicker compared with animals, and therefore optimal intensity of physical agents that induce bone adaptation in human may differ. In particular, up to 40% of ultrasound exergy is reflected at the soft tissue–bone interface [22, 23]. Therefore, further studies are warranted to explore the effects of physical agents on postmenopausal women. Second, our study showed that physical agents improve local bone turnover, but their systemic effects are at present unknown. Finally, these findings may be unique to estrogen deficiency-induced osteoporosis, and whether they can be applied to other bone conditions, such as healthy bone or unloading, steroid, or aging-induced osteoporosis, could be ascertained in further studies.

In conclusion, we demonstrated that mechanical stress induced by radial extracorporeal shock wave and ultrasound improved trabecular bone loss and bone fragility caused by estrogen deficiency via osteoblast activation or osteoclast inactivation. Furthermore, our findings suggest that exposure of ultrasound at higher intensity (1.5 W/cm^2) induces osteocyte mechano-transduction and results in bone formation. We propose that radial extracorporeal shock wave and ultrasound are easy and noninvasive as a promising nonpharmacologic therapy for osteoporosis; future studies should explore its clinical application.

Supplementary Information The online version contains supplementary material available at https://doi.org/10.1007/s00223-021-00831-6.

Acknowledgements We thank Mr. Masato Nomura, Mr. Yoshio Wakimoto, Mr. Ryota Suzuki, Mr. Takumi Yakuwa, Mr. Changxin Li, Mr. Taisei Wakigawa, Mr. Toshiya Tsubaki, and Ms. Sae Kinoshita for their skilled technical assistance; Asst. Prof. Akira Ito and Dr. Akihiro Nakahata for their support with mechanical testing; and Asst. Prof. Noriaki Maeshige for support with the ultrasound transducer. We are also grateful to Nihon Medix Co., Ltd. for providing the electrical stimulator; and SAKAI Medical Co., Ltd. for providing the radial extracorporeal shock wave device.

Funding This work was supported by the Japan Society for the Promotion of Science KAKENHI Grant No. 16K12933 and Suzuken Memorial Foundation.

Data Availability The datasets used and analyzed during this study are available from corresponding author upon request.

Declarations

Conflict of interest Shota Inoue, Junpei Hatakeyama, Hitoshi Aoki, Hiroshi Kuroki, Takahiro Niikura, Keisuke Oe, Tomoaki Fukui, Ryosuke Kuroda, Toshihiro Akisue, and Hideki Moriyama declare that they have no conflict of interest.

Ethical approval All experimental procedures were approved by the Institutional Animal Care and Use Committee and performed according to the Kobe University Animal Experimentation Regulations (approval number: P160607).

Informed consent For this type of study, no informed consent is required.

References

1. NIH Consensus Development Panel on Osteoporosis Prevention, Diagnosis, and Therapy (2001) Osteoporosis Prevention, Diagnosis, and Therapy. JAMA 285(6):785–795
2. Lips P, van Schoor NM (2005) Quality of life in patients with osteoporosis. Osteoporos Int 16:447–455. https://doi.org/10.1007/s00198-004-1762-7
3. Ensrud KE, Thompson DE, Cauley JA, Nevitt MC, Kado DM, Hochberg MC, Santora AC et al (2000) Prevalent vertebral deformities predict mortality and hospitalization in older women with low bone mass. J Am Geriatr Soc 48:241–249. https://doi.org/10.1111/j.1532-5415.2000.tb02641.x
4. McClung M, Harris ST, Miller PD, Bauer DC, Davison KS, Dian L, Hanley DA et al (2013) Bisphosphonate therapy for

osteoporosis: benefits, risks, and drug holiday. Am J Med 126:13–20. https://doi.org/10.1016/j.amjmed.2012.06.023
5. Bilezikian JP (2006) Osteonecrosis of the jaw - do bisphosphonates pose a risk? N Engl J Med 355:2278–2281. https://doi.org/10.1056/NEJMp068157
6. Kohrt WM, Bloomfield SA, Little KD, Nelson ME, Yingling VR (2004) Physical activity and bone health. Med Sci Sports Exerc 36:1985–1996. https://doi.org/10.1249/01.MSS.0000142662.21767.58
7. Moreira LDF, de Oliveira ML, Lirani-Galvão AP, Marin-Mio RV, dos Santos RN, Lazaretti-Castro M (2014) Physical exercise and osteoporosis: effects of different types of exercises on bone and physical function of postmenopausal women. Arq Bras Endocrinol Metabol 58:514–522. https://doi.org/10.1590/0004-2730000003374
8. Duncan RL, Turner CH (1995) Mechanotransduction and the functional response of bone to mechanical strain. Calcif Tissue Int 57:344–358. https://doi.org/10.1007/BF00302070
9. Turner CH (1998) Three rules for bone adaptation to mechanical stimuli. Bone 23:399–407. https://doi.org/10.1016/S8756-3282(98)00118-5
10. Robling AG, Niziolek PJ, Baldridge LA, Condon KW, Allen MR, Alam I, Mantila SM et al (2008) Mechanical stimulation of bone in vivo reduces osteocyte expression of Sost/sclerostin. J Biol Chem 283:5866–5875. https://doi.org/10.1074/jbc.M705092200
11. Lam H, Qin Y-X (2008) The effects of frequency-dependent dynamic muscle stimulation on inhibition of trabecular bone loss in a disuse model. Bone 43:1093–1100. https://doi.org/10.1016/j.bone.2008.07.253
12. Midura RJ, Dillman CJ, Grabiner MD (2005) Low amplitude, high frequency strains imposed by electrically stimulated skeletal muscle retards the development of osteopenia in the tibiae of hindlimb suspended rats. Med Eng Phys 27:285–293. https://doi.org/10.1016/j.medengphy.2004.12.014
13. Jee WS, Yao W (2001) Overview: animal models of osteopenia and osteoporosis. J Musculoskelet Neuronal Interact 1:193–207
14. Wang CJ, Yang KD, Wang FS, Hsu CC, Chen HH (2004) Shock wave treatment shows dose-dependent enhancement of bone mass and bone strength after fracture of the femur. Bone 34:225–230. https://doi.org/10.1016/j.bone.2003.08.005
15. Rompe JD, Rosendahl T, Schöllner C, Theis C (2001) High-energy extracorporeal shock wave treatment of nonunions. Clin Orthop Relat Res. https://doi.org/10.1097/00003086-200106000-00014
16. Van Der Jagt OP, Van Der Linden JC, Schaden W, Van Schie HT, Piscaer TM, Verhaar JAN, Weinans H et al (2009) Unfocused extracorporeal shock wave therapy as potential treatment for osteoporosis. J Orthop Res 27:1528–1533. https://doi.org/10.1002/jor.20910
17. Van Der Jagt OP, Waarsing JH, Kops N, Schaden W, Jahr H, Verhaar JAN, Weinans H (2013) Unfocused extracorporeal shock waves induce anabolic effects in osteoporotic rats. J Orthop Res 31:768–775. https://doi.org/10.1002/jor.22258
18. Koolen MKE, Kruyt MC, Öner FC, Schaden W, Weinans H, van der Jagt OP (2019) Effect of unfocused extracorporeal shockwave therapy on bone mineral content of twelve distal forearms of postmenopausal women: a clinical pilot study. Arch Osteoporos. https://doi.org/10.1007/s11657-019-0650-x
19. Watanabe Y, Matsushita T, Bhandari M, Zdero R, Schemitsch EH (2010) Ultrasound for fracture healing: current evidence. J Orthop Trauma 24:S56–S61. https://doi.org/10.1097/BOT.0b013e3181d2efaf
20. Lim D, Ko CY, Seo DH, Woo DG, Kim JM, Chun KJ, Kim HS (2011) Low-intensity ultrasound stimulation prevents osteoporotic bone loss in young adult ovariectomized mice. J Orthop Res 29:116–125. https://doi.org/10.1002/jor.21191
21. Ferreri SL, Talish R, Trandafir T, Qin Y-X (2011) Mitigation of bone loss with ultrasound induced dynamic mechanical signals in an OVX induced rat model of osteopenia. Bone 48:1095–1102. https://doi.org/10.1016/j.bone.2011.01.002
22. Warden SJ, Bennell KL, Forwood MR, McMeeken JM, Wark JD (2001) Skeletal effects of low-intensity pulsed ultrasound on the ovariectomized rodent. Ultrasound Med Biol 27:989–998. https://doi.org/10.1016/S0301-5629(01)00376-3
23. Warden SJ, Bennell KL, Matthews B, Brown DJ, McMeeken JM, Wark JD (2001) Efficacy of low-intensity pulsed ultrasound in the prevention of osteoporosis following spinal cord injury. Bone 29:431–436. https://doi.org/10.1016/S8756-3282(01)00599-3
24. Leung KS, Lee WS, Cheung WH, Qin L (2004) Lack of efficacy of low-intensity pulsed ultrasound on prevention of postmenopausal bone loss evaluated at the distal radius in older Chinese women. Clin Orthop Relat Res. https://doi.org/10.1097/01.blo.0000137557.59228.4d
25. Angle SR, Sena K, Sumner DR, Virdi AS (2011) Osteogenic differentiation of rat bone marrow stromal cells by various intensities of low-intensity pulsed ultrasound. Ultrasonics 51:281–288. https://doi.org/10.1016/j.ultras.2010.09.004
26. Li JGR, Chang WHS, Lin JCA, Sun JS (2002) Optimum intensities of ultrasound for PGE2 secretion and growth of osteoblasts. Ultrasound Med Biol 28:683–690. https://doi.org/10.1016/S0301-5629(02)00485-4
27. Kalu DN (1991) The ovariectomized rat model of postmenopausal bone loss. Bone Miner 15:175–191. https://doi.org/10.1016/0169-6009(91)90124-I
28. Stürmer EK, Seidlová-Wuttke D, Sehmisch S, Rack T, Wille J, Frosch KH, Wuttke W et al (2006) Standardized bending and breaking test for the normal and osteoporotic metaphyseal tibias of the rat: Effect of estradiol, testosterone, and raloxifene. J Bone Miner Res 21:89–96. https://doi.org/10.1359/JBMR.050913
29. Kawamoto T (2003) Use of a new adhesive film for the preparation of multi-purpose fresh-frozen sections from hard tissues, whole-animals, insects and plants. Arch Histol Cytol 66:123–143. https://doi.org/10.1679/aohc.66.123
30. McKenzie J, Smith C, Karuppaiah K, Langberg J, Silva MJ, Ornitz DM (2019) Osteocyte death and bone overgrowth in mice lacking fibroblast growth factor receptors 1 and 2 in mature osteoblasts and osteocytes. J Bone Miner Res 34:1660–1675. https://doi.org/10.1002/jbmr.3742
31. Moriyama H, Kanemura N, Brouns I, Pintelon I, Adriaensen D, Timmermans JP, Ozawa J et al (2012) Effects of aging and exercise training on the histological and mechanical properties of articular structures in knee joints of male rat. Biogerontology 13:369–381. https://doi.org/10.1007/s10522-012-9381-8
32. Nomura M, Sakitani N, Iwasawa H, Kohara Y, Takano S, Wakimoto Y, Kuroki H et al (2017) Thinning of articular cartilage after joint unloading or immobilization. An experimental investigation of the pathogenesis in mice. Osteoarthr Cartil 25:727–736. https://doi.org/10.1016/j.joca.2016.11.013
33. Kaneguchi A, Ozawa J, Kawamata S, Yamaoka K (2017) Development of arthrogenic joint contracture as a result of pathological changes in remobilized rat knees. J Orthop Res 35:1414–1423. https://doi.org/10.1002/jor.23419
34. Livak KJ, Schmittgen TD (2001) Analysis of relative gene expression data using real-time quantitative PCR and the 2-ΔΔCT method. Methods 25:402–408. https://doi.org/10.1006/meth.2001.1262
35. Faul F, Erdfelder E, Lang A-G, Buchner A (2007) G*Power 3: a flexible statistical power analysis program for the social, behavioral, and biomedical sciences. Behav Res Methods 39:175–191. https://doi.org/10.3758/BF03193146

36. McElroy JF, Wade GN (1987) Short- and long-term effects of ovariectomy on food intake, body weight, carcass composition, and brown adipose tissue in rats. Physiol Behav 39:361–365. https://doi.org/10.1016/0031-9384(87)90235-6
37. Tella SH, Gallagher JC (2014) Prevention and treatment of postmenopausal osteoporosis. J Steroid Biochem Mol Biol 142:155–170. https://doi.org/10.1016/j.jsbmb.2013.09.008
38. Wronski TJ, Lowry PL, Walsh CC, Ignaszewski LA (1985) Skeletal alterations in ovariectomized rats. Calcif Tissue Int 37:324–328. https://doi.org/10.1007/BF02554882
39. Turner CH, Burr DB (1993) Basic biomechanical measurements of bone: A tutorial. Bone 14:595–608. https://doi.org/10.1016/8756-3282(93)90081-K
40. Wronski TJ, Cintrón M, Dann LM (1988) Temporal relationship between bone loss and increased bone turnover in ovariectomized rats. Calcif Tissue Int 43:179–183. https://doi.org/10.1007/BF02571317
41. Gerstenfeld LC, Chipman SD, Glowacki J, Lian JB (1987) Expression of differentiated function by mineralizing cultures of chicken osteoblasts. Dev Biol 122:49–60. https://doi.org/10.1016/0012-1606(87)90331-9
42. Minkin C (1982) Bone acid phosphatase: tartrate-resistant acid phosphatase as a marker of osteoclast function. Calcif Tissue Int 34:285–290. https://doi.org/10.1007/BF02411252
43. Wada T, Nakashima T, Hiroshi N, Penninger JM (2006) RANKL-RANK signaling in osteoclastogenesis and bone disease. Trends Mol Med 12:17–25. https://doi.org/10.1016/j.molmed.2005.11.007
44. Bonewald LF (2011) The amazing osteocyte. J Bone Miner Res 26:229–238. https://doi.org/10.1002/jbmr.320
45. Jilka RL, Noble B, Weinstein RS (2013) Osteocyte apoptosis. Bone 54:264–271. https://doi.org/10.1016/j.bone.2012.11.038
46. Tomkinson A, Gevers EF, Wit JM, Reeve J, Noble BS (1998) The role of estrogen in the control of rat osteocyte apoptosis. J Bone Miner Res 13:1243–1250. https://doi.org/10.1359/jbmr.1998.13.8.1243
47. Verborgt O, Tatton NA, Majeska RJ, Schaffler MB (2002) Spatial distribution of Bax and Bcl-2 in osteocytes after bone fatigue: complementary roles in bone remodeling regulation? J Bone Miner Res 17:907–914. https://doi.org/10.1359/jbmr.2002.17.5.907
48. Delius M, Draenert K, Al Diek Y, Draenert Y (1995) Biological effects of shock waves: In vivo effect of high energy pulses on rabbit bone. Ultrasound Med Biol 21:1219–1225. https://doi.org/10.1016/0301-5629(95)00030-5
49. Sapir-Koren R, Livshits G (2014) Osteocyte control of bone remodeling: is sclerostin a key molecular coordinator of the balanced bone resorption–formation cycles? Osteoporos Int 25:2685–2700. https://doi.org/10.1007/s00198-014-2808-0